Transportation Research Part C 62 (2016) 87–102

Contents lists available at ScienceDirect

Transportation Research Part C

journal homepage: www.elsevier.com/locate/trc

A dynamic automated lane change maneuver based on vehicle-to-vehicle communication

Yugong Luo *, Yong Xiang, Kun Cao, Keqiang Li

State Key Laboratory of Automotive Safety and Energy, Tsinghua University, Beijing 100084, PR China

ARTICLE INFO

Article history:
Received 2 April 2015
Received in revised form 26 November 2015
Accepted 26 November 2015
Available online 15 December 2015

Keywords:
Automated lane change
Vehicle-to-vehicle communication
Trajectory planning
Trajectory tracking
Constrained optimization

ABSTRACT

Automated driving is gaining increasing amounts of attention from both industry and academic communities because it is regarded as the most promising technology for improving road safety in the future. The ability to make an automated lane change is one of the most important parts of automated driving. However, there has been little research into automated lane change maneuvers, and current research has not identified a way to avoid potential collisions during lane changes, which result from the state variations of the other vehicles. One important reason is that the lane change vehicle cannot acquire accurate information regarding the other vehicles, especially the vehicles in the adjacent lane. However, vehicle-to-vehicle communication has the advantage of providing more information, and this information is more accurate than that obtained from other sensors, such as radars and lasers. Therefore, we propose a dynamic automated lane change maneuver based on vehicle-to-vehicle communication to accomplish an automated lane change and eliminate potential collisions during the lane change process. The key technologies for this maneuver are trajectory planning and trajectory tracking. Trajectory planning calculates a reference trajectory satisfying the demands of safety, comfort and traffic efficiency and updates it to avoid potential collisions until the lane change is complete. The trajectory planning method converts the planning problem into a constrained optimization problem using the lane change time and distance. This method is capable of planning a reference trajectory for a normal lane change, an emergency lane change and a change back to the original lane. A trajectory-tracking controller based on sliding mode control calculates the control inputs to make the host vehicle travel along the reference trajectory. Finally, simulations and experiments using a driving simulator are conducted. They demonstrate that the proposed dynamic automated lane change maneuver can avoid potential collisions during the lane change process effectively.

1. Introduction

Automated driving is considered as a promising solution to improve road safety in the future, and research on this subject is gathering increasing attention (Hatipoglu et al., 1997; Carbaugh et al., 1998; Girault, 2004; Tideman et al., 2010; Fraedrich and Lenz, 2014). Research about automated lane following is found in many studies (Adell et al., 2011). In contrast, little research about automated lane changes has been undertaken; however, the automated lane change is a necessary part for automated driving. Because lane change is not only the reason for 4–10% of all the accidents, but also cause for 10% of the latencies on roads (Ammoun et al., 2007).

* Corresponding author. Tel.: +86 010 62784462.
E-mail address: lyg@mail.tsinghua.edu.cn (Y. Luo).

http://dx.doi.org/10.1016/j.trc.2015.11.011
0968-090X/

(Hidas, 2002) presented lane-changing models in a microscopic traffic network and developed an intelligent concept for lane changing and merging. However, the models are based on autonomous agent concept, which is far different from the real car. Zheng (2014) summarized two kinds of models about the lane change decision-making and lane change impact in detail. It is useful to have a better understanding of the lane change. However, the paper did not deal with the maneuver that guarantees an automated lane change. Chee and Tomizuka (1994a,b) and Chee et al. (1995a,b) studied automated lane change maneuvers including a comparison of four different desired trajectories and two trajectory-tracking algorithms. They selected a trapezoidal acceleration trajectory as the virtual desired trajectory and showed that the sliding mode controller was better at stabilizing the system. However, they considered lane-changing vehicle in isolation. Hatipoglu et al. (1995) designed an optimal lane change controller. The closed-loop system with respect to a certain optimality criterion led to a smoother and slightly delayed response compared to the open-loop system. A closed-loop lane change maneuver can be accomplished on curved roads in the same manner. Sledge and Marshek (1997) compared six candidate lane-change trajectories based on selected criteria. The comparison was treated as an optimization problem with prescribed continuity and boundary conditions, in which the length, curvature, and rate of change of curvature were taken as its costs. The maximum constant velocity was employed as an additional discriminator. The comparison showed that a quintic polynomial is the simpler of the two best lane-change trajectory functions. Papadimitriou and Tomizuka (2003) employed quintic polynomial to compute a lane change trajectory. Their trajectory treated obstacles as simplified s-topes and dynamic constraints were taken into consideration. The criterion for selecting the desired and achievable trajectory involved the choice of a single coefficient. This strategy can only handle obstacles at the starting instant; it cannot address obstacles that appear during the lane change process. Wan et al. (2011) introduced an algorithm for an automated lane change maneuver based on recognition of the surroundings. The algorithm employed on-board sensors for signals such as the speed of each vehicle and the relative distances between vehicles and estimated the final positions of the host and surrounding vehicles after the lane change maneuver. Wang et al. (2015) focused on the lane-change decision-making during the car following control, however, it did not pay much attention to the lane change process and just employed a simple lane-change reference trajectory, which did not consider the lateral speed and yaw rate of the lane-change vehicle. To the best of our knowledge, current research has not found a way to handle the potential of a collision occurring during the lane change process, and the existing trajectory planning methods have their limitations when dynamically planning a reference trajectory. One of the reasons is that on-board sensors cannot acquire information on the vehicles in the adjacent lane accurately.

However, with the development of vehicle-to-vehicle communication, which equips the vehicles with ability to communicate with each other, and its benefits, which include a larger perception range, more accurate information and more kinds of information (Ammoun and Nashashibi, 2010; Guan et al., 2011; Greg, 2014). With vehicle-to-vehicle communication, we can obtain more information about the surroundings and the available information is more accurate. A variety of applications in vehicle safety have already been developed (Kato et al., 2002; Gallagher et al., 2006; Misener, 2008; Williams et al., 2012; Hu et al., 2012).

With the help of vehicle-to-vehicle communication, the position, speed and acceleration of the vehicles in the adjacent lane can be acquired more accurately. Therefore, we design our automated lane change maneuver based on vehicle-to-vehicle communication.

The contributions of this paper are:

(1) The problem of how to avoid potential collisions occurring during the automated lane changing process is solved through a universal automated lane change maneuver. Other previous studies have seldom considered potential collisions during lane changes; in this paper, we employ minimum safety spacing as a guarantee of safety in the automated lane change process. With these criteria, the dynamic automated lane change maneuver adjusts its reference trajectory according to the environment with the help of vehicle-to-vehicle communication. It maintains a sufficient distance between the host vehicle and the other vehicles to avoid any type of collision. The dynamic automated lane change maneuver is not a special maneuver that is effective only for potential collision avoidance. It can also guarantee a smooth automated lane change when there is no potential collision threaten.

(2) The trajectory planning method is a universal method that can be applied to different scenarios. It takes safety, comfort and traffic efficiency into account. It employs a quintic polynomial as the trajectory function and the problem is converted into a constrained optimization problem based on the lane change time and distance. When the boundary conditions are updated as constraints, we update the reference trajectory. Therefore, this trajectory planning method can plan not only a reference trajectory in which the other vehicles maintain their states but also one in which the states of the other vehicles vary. In particular, it can plan a reference trajectory during the lane change that makes the host vehicle return to the original lane.

The rest of the paper is organized as follows. Section 2 describes the design of the dynamic automated lane change maneuver, which includes trajectory planning and trajectory tracking; Section 3 provides the results of simulations and experiments on automated lane changes in several typical scenarios, and Section 4 presents the paper's conclusions.

2. A dynamic automated lane change maneuver

An automated lane change maneuver should be carefully designed by considering a variety of factors, including safety and comfort. The proposed dynamic automated lane change maneuver has the structure shown in Fig. 1.

The maneuver consists of two parts, trajectory planning and trajectory tracking. To plan the trajectory, the current state (position, speed, acceleration and so on) of the vehicle and environmental information, including the states of other vehicles, are necessary. The information is collected using sensors and vehicle-to-vehicle communication. There is already a significant amount of research into the design and application of vehicle-to-vehicle communication (Tian and Leung, 2011; Liu et al., 2012; Tian et al., 2013, 2014; Wang et al., 2013).

The trajectory planning part of the maneuver generates a reference trajectory satisfying the demands of safety, comfort and traffic efficiency. This trajectory is calculated by establishing a proper cost function and satisfying related constraints and converting the problem into a constrained optimization problem.

The trajectory tracking part of the maneuver controls the system based on the tracking errors between the current trajectory and the reference trajectory. To implement the desired control and make the vehicle follow the reference trajectory, it should be converted into actuators' input.

2.1. A polynomial trajectory planning method

Planning a reference trajectory before changing lane is both necessary and important. The quality of the reference trajectory has a direct impact on the performance of the automated lane change. Therefore, safety, comfort and traffic efficiency are considered when planning the reference trajectory.

2.1.1. Performance specification of the lane change trajectory

(1) Safety

The most important goal of an automated lane change is safety. The relative positions between the host vehicle and the other vehicles in a typical lane change scenario are shown in Fig. 2. We consider only the four vehicles closest to the host vehicle (M), i.e., the leading vehicle on the destination lane (L_d), the following vehicle on the destination lane (F_d), the leading vehicle on the original lane (L_o), and the following vehicle on the original lane (F_o).

Usually, three factors should be considered to ensure safety.

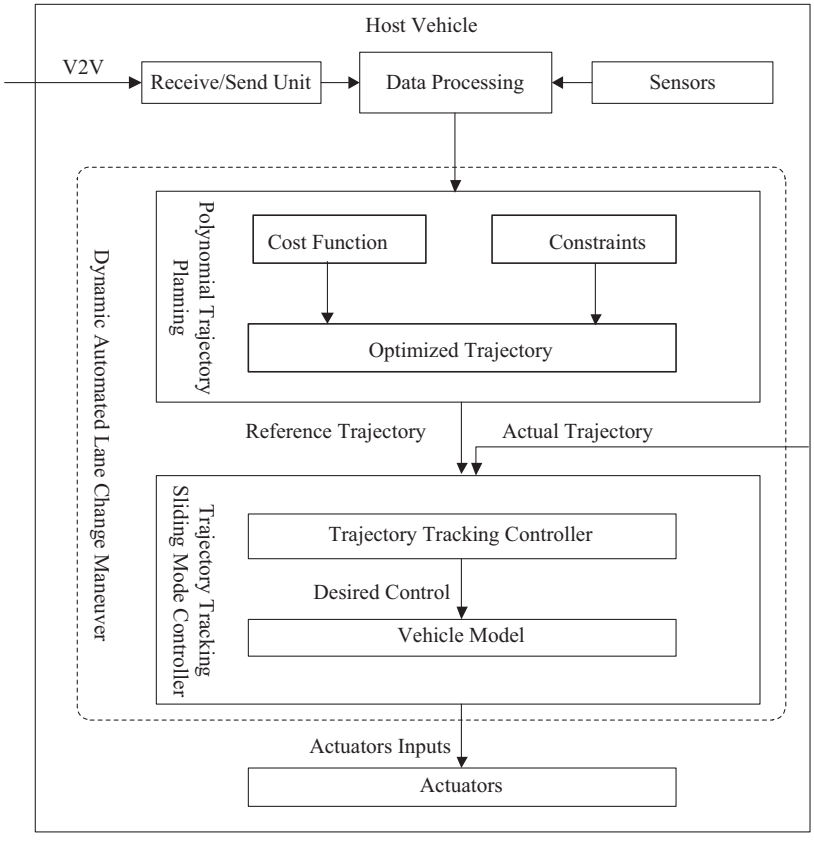

Fig. 1. The structure of the dynamic automated lane change maneuver.

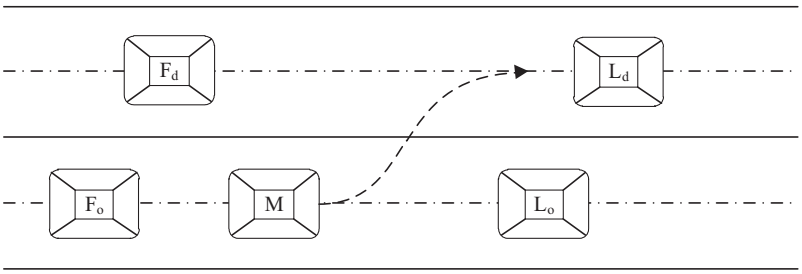

Fig. 2. The relative position of the host vehicle and the other vehicles.

(a) Position limitation

First, the host vehicle should not travel beyond the border of the road. During a lane change, the host vehicle should stay between the two lane centers.

$$0 < y(t) < w, \quad \forall t \in [0, t_f] \tag{1}$$

where $y(t)$ is the lateral position of the host vehicle at the time t, w is the lane width, t_f is the lane change time duration.

(b) Speed limitation

Second, the longitudinal speed of the host vehicle should not exceed the maximum allowable speed on the current road and it should always be positive, i.e., no stop or backward displacement.

$$0 < v_x(t) < v_{x,max} \tag{2}$$

where $v_x(t)$ is the longitudinal speed of the host vehicle at the time t, $v_{x,max}$ is the maximum allowable speed on the current road.

(c) Potential collision avoidance

Last, the host vehicle should maintain a sufficient distance from other vehicles when setting up the automated lane change maneuver to avoid potential collisions during the lane change. Because of the low latency of vehicle-to-vehicle communication, the host vehicle can quickly react to the other vehicles' states. The host vehicle can keep its distance from other vehicles as short as possible when it drives along the road (in this paper, we assume a distance of 3 m between the host vehicle and any other vehicle). Here, the minimum safety spacing is employed to describe the premise for a collision-free lane change (Jula et al., 2000). The minimum safety spacings between H and L_d, F_d, L_o, and F_o are calculated by the following formulas:

$$MSS(M, L_d) = \max\left(\int_0^t \int_0^\lambda (a_M(\tau) - a_{L_d}(\tau))d\tau d\lambda + (v_M(0) - v_{L_d}(0))t\right) \quad \forall t \in [t_C, t_f] \tag{3}$$

$$MSS(M, F_d) = \max\left(\int_0^t \int_0^\lambda (a_{F_d}(\tau) - a_M(\tau))d\tau d\lambda + (v_{F_d}(0) - v_M(0))t\right) \quad \forall t \in [t_C, t_f] \tag{4}$$

$$MSS(M, L_o) = \max\left(\int_0^t \int_0^\lambda (a_M(\tau) - a_{L_o}(\tau))d\tau d\lambda + (v_M(0) - v_{L_o}(0))t\right) \quad \forall t \in [0, t_C] \tag{5}$$

$$MSS(M, F_o) = \max\left(\int_0^t \int_0^\lambda (a_{F_o}(\tau) - a_M(\tau))d\tau d\lambda + (v_{F_o}(0) - v_M(0))t\right) \quad \forall t \in [0, t_C] \tag{6}$$

where a_i and v_i are the acceleration and speed of each vehicle, $i \in \{M, L_d, F_d, L_o, F_o\}$, and t_C is the instant when the host vehicle reaches the critical point C, which is the first potential collision point between the host vehicle and the other vehicle when the host vehicle enters the destination lane.

The minimum safety spacings calculated in (3)–(6) are not the only criteria used to decide if the lane change process is safe or not; they are also used to ensure that the planned optimized lane change trajectory will not result in a collision as constraint in (23). When there are no other vehicles, there is no need to consider the minimum safety spacing, so the constraints in (3)–(6) are ignored. The constraints become effective when there are other vehicles and the safety condition is not satisfied. Not only at the start of the lane change, but also at any instant after the lane change is initiated, the constraints of the distances between the host vehicle and the other vehicles guarantee that a feasible reference trajectory results in a safe lane change. When a potential collision appears after the lane change is initiated, the constraints update themselves accord-

ing to the new environment. A new reference trajectory subject to the new constraints is computed. With this new reference trajectory the potential collision after the lane change is initiated can also be effectively avoided.

The new reference trajectory avoids the potential collision, which is how the dynamic automated lane change trajectory avoids potential collisions.

(2) Comfort

To guarantee a comfortable lane change, the accelerations and jerks in both directions should not be too great.

$$|a_x| < a_{x,max} \tag{7}$$

$$|a_y| < a_{y,max} \tag{8}$$

$$|j_x| < j_{x,max} \tag{9}$$

$$|j_y| < j_{y,max} \tag{10}$$

where $a_{x,max}$ is the maximum allowable longitudinal acceleration, $a_{y,max}$ is the maximum allowable lateral acceleration, $j_{x,max}$ is the maximum allowable longitudinal jerk, and $j_{y,max}$ is the maximum allowable lateral jerk.

Jerk is one of the most important factors affecting ride comfort. As we know, passengers feel no force when a vehicle moves at constant speed. In addition, passengers can adjust themselves to forces resulting from constant acceleration. However, passengers will lose equilibrium when the acceleration varies, i.e., when the jerk is non-zero. Therefore, to improve ride comfort, the jerks in both directions should be as small as possible (Hult and Tabar, 2013).

$$\min J_1 = w_1 \int_0^{t_f} j_x^2(\tau)d\tau + w_2 \int_0^{t_f} j_y^2(\tau)d\tau \tag{11}$$

where w_1 and w_2 are weight factors.

(3) Traffic efficiency

Because changing lane involves at least two adjacent lanes, it will have an effect on the motion of the vehicles in both lanes, which may reduce the traffic efficiency. Minimizing the length of the lane change, x_f, will decrease its impact on the traffic efficiency.

$$\min J_2 = x_f \tag{12}$$

2.1.2. Trajectory planning problem description

(1) Trajectory planning on a straight road

To model the trajectory of a lane change, a suitable trajectory function should be selected. Here we choose the quintic polynomial based on time, which has the advantages of a closed form, a continuous third derivative and smooth curvature.

$$\begin{cases} x(t) = a_5t^5 + a_4t^4 + a_3t^3 + a_2t^2 + a_1t + a_0 \\ y(t) = b_5t^5 + b_4t^4 + b_3t^3 + b_2t^2 + b_1t + b_0 \end{cases} \tag{13}$$

Twelve unknown coefficients must be determined in the above functions. With considering the boundary conditions of the lane change process, i.e., the initial state of the lane change trajectory corresponds to the current state of the host vehicle and the final state is the same as the desired state for the host vehicle, as shown in (14) and (15).

$$\begin{cases} x(0) = x_0,\ \dot{x}(0) = v_{x,0},\ \ddot{x}(0) = a_{x,0} \\ y(0) = y_0,\ \dot{y}(0) = v_{y,0},\ \ddot{y}(0) = a_{y,0} \end{cases} \tag{14}$$

$$\begin{cases} x(t_f) = x_f,\ \dot{x}(t_f) = v_{x,f},\ \ddot{x}(t_f) = a_{x,f} \\ y(t_f) = y_f,\ \dot{y}(t_f) = v_{y,f},\ \ddot{y}(t_f) = a_{y,f} \end{cases} \tag{15}$$

where x_0 and y_0 are the current longitudinal and lateral coordinates, $v_{x,0}$ and $v_{y,0}$ are the current longitudinal and lateral velocities, and $a_{x,0}$ and $a_{y,0}$ are the current longitudinal and lateral accelerations. We assume that the host vehicle travels at constant speed along the centerline of the destination lane when it finishes the lane change. The final lateral position y_f is one lane-width from the current position, the final longitudinal speed $v_{x,f}$ is the average speed of the destination lane, and the lateral speed $v_{y,f}$ and the longitudinal and lateral accelerations $a_{x,f}$ and $a_{y,f}$ are zero. However, the lane change time t_f and distance x_f are not easy to determine and it is unreasonable simply to assign arbitrary values to them, as performed in most studies (Nelson, 1989; Ammoun et al., 2007).

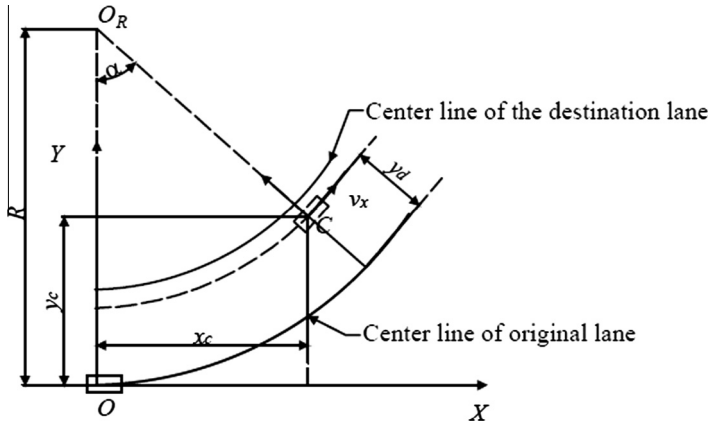

Fig. 3. A lane change on a curved road.

We treat the lane change time t_f and lane change distance x_f as free variables. With the boundary conditions, the unknown coefficients in the trajectory function can be represented as functions of t_f and x_f. Therefore, the problem of finding the unknown coefficients is converted into the problem of determining the lane change time t_f and distance x_f.

The cost function of lane change trajectory must be minimized subject to certain constraints as discussed above. Therefore, the problem planning a trajectory for an automated lane change can be converted into the constrained optimization problem shown in (16)–(23).

$$\min\ J(t_f, x_f) = w_1 \frac{\int_0^{t_f} j_x^2(\tau)d\tau}{j_{x,max} a_{x,max}} + w_2 \frac{\int_0^{t_f} j_y^2(\tau)d\tau}{j_{y,max} a_{y,max}} + w_3 \frac{x_f}{kw} \tag{16}$$

s.t.

$$0 < y(t) < w \tag{17}$$

$$0 < \sqrt{\dot{x}^2(t) + \dot{y}^2(t)} < v_{max} \tag{18}$$

$$|\ddot{x}(t)| < a_{x,max} \tag{19}$$

$$|\ddot{y}(t)| < a_{y,max} \tag{20}$$

$$|\dddot{x}(t)| < j_{x,max} \tag{21}$$

$$|\dddot{y}(t)| < j_{y,max} \tag{22}$$

$$MSS(M,i) + d_0 < d(M,i) \tag{23}$$

where w_3 is a weight factor, k is a constant, w is the lane width, M is the host vehicle, i can be any one of the four nearest vehicles, L_d, F_d, L_o, and F_o, d_0 is the safety distance allowance.

(2) Trajectory planning on a curved road

The above trajectory is obtained on the straight roads, but can also be applied on the curved roads with some adaptation. The vehicle's motion on a curved road can be treated as the superposition of its linear motion and its circular motion around the instantaneous center of the road's curvature. Using the geometric relationship shown in Fig. 3, we find that the lane change trajectory on a curved road is

$$x(t) = [R - y_d(t)] \sin\alpha \tag{24}$$

$$y(t) = R - [R - y_d(t)] \cos\alpha \tag{25}$$

where R is the radius of curvature of the road and $\alpha = \int_0^t \frac{v_x}{R - y_d(\tau)} d\tau$ is the angle the vehicle rotates around the instantaneous center of curvature.

2.1.3. Solving the problem

To solve the constrained optimization problem, the interior-point algorithm is employed. This algorithm converts the constrained minimization problem in (26) into the sequence of approximate minimization problems shown in (27).

$$\begin{aligned} \min_{x} \quad & f(x) \\ \text{s.t.} \quad & h(x) = 0 \\ & g(x) \le 0 \end{aligned} \tag{26}$$

where $f(x)$ is the cost function, $h(x)$ is the equality constraint, and $g(x)$ is the inequality constraint.

$$\begin{aligned} \min_{x,s} \quad & f_\mu(x,s) = \min_{x,s} f(x) - \mu \sum_i \ln(s_i) \\ \text{s.t.} \quad & h(x) = 0 \\ & g(x) + s = 0 \end{aligned} \tag{27}$$

There are as many slack variables s_i as there are inequality constraints g and the s_i are required to be positive. As μ decreases to zero, the minimum of f_μ should approach the minimum of f.

To solve the approximate problem, the algorithm employs one of two main types of steps at each iteration. A direct step in (x, s) attempts to solve the KKT equations in (29) for the approximate problem via a linear approximation. A CG (conjugate gradient) step employs a trust region. The algorithm tries a direct step first and tries a CG step if there is no feasible step from the direct step.

The direct step constructs the Lagrangian first.

$$L(x,s,\lambda,y) = f(x) - \mu \sum_i \ln(s_i) + \sum_i \lambda_i (g_i(x) + s_i) + \sum_j y_j h_j(x) \tag{28}$$

$$\begin{cases} \nabla_x L(x,s,\lambda,y) = 0 \\ \lambda_i g_i(x) = 0 \quad \forall i \end{cases} \tag{29}$$

The iteration step $(\Delta x, \Delta s)$ is solved as follows:

$$\begin{bmatrix} H & 0 & J_h^T & J_g^T \\ 0 & S\Lambda & 0 & -S \\ J_h & 0 & I & 0 \\ J_g & -S & 0 & I \end{bmatrix} \begin{bmatrix} \Delta x \\ \Delta s \\ -\Delta y \\ -\Delta \lambda \end{bmatrix} = - \begin{bmatrix} \nabla f - J_h^T y - J_g^T \lambda \\ S\lambda - \mu e \\ h \\ g + s \end{bmatrix} \tag{30}$$

$$H = \nabla^2 f(x) - \mu \sum_i \nabla^2 \ln(s_i) + \sum_i \lambda_i \nabla^2 g_i(x) + \sum_j y_j \nabla^2 h_j(x) \tag{31}$$

where H denotes the Hessian of the Lagrangian of f_μ, J_g denotes the Jacobian of constraint function g, J_h denotes the Jacobian of constraint function h, $S = \text{diag}(s)$, λ denotes the Lagrange multiplier vector associated with constraint g, $\Lambda = \text{diag}(\lambda)$, y denotes the Lagrange multiplier vector associated with h, and e denotes the vector of ones with the same size as g.

The CG approach is to minimize a quadratic approximation in (32) to the approximate problem in a trust region, subject to the linearized constraints shown in (33).

$$\min_{\Delta x, \Delta s} \nabla f^T \Delta x + \frac{1}{2} \Delta x^T \nabla_{xx}^2 L(x,s,\lambda,y) \Delta x + \mu e^T S^{-1} \Delta s + \frac{1}{2} \Delta s^T S^{-1} \Lambda \Delta s \tag{32}$$

$$\begin{aligned} \text{s.t.} \quad & g(x) + J_g \Delta x + \Delta s = 0 \\ & h(x) + J_h \Delta x = 0 \end{aligned} \tag{33}$$

By solving the constrained optimization problem with the interior-point algorithm, we find the optimal lane change time t_f and distance x_f. The optimal solution makes the jerk as small as possible and the lane change distance as short as possible while satisfying the condition of minimum safety spacing. Therefore, safety, comfort and traffic efficiency are well balanced.

2.2. A trajectory-tracking sliding mode controller

To complete the automated lane change as expected, we must make the host vehicle travel along the designed reference trajectory. We design a controller for trajectory tracking based on sliding mode control.

In the design process, we treat the host vehicle as a rigid object with the same dimensions. The differences between the actual trajectory and the reference trajectory are characterized by the longitudinal and lateral coordinates of the vehicle and its heading angle, which are shown in Fig. 4.

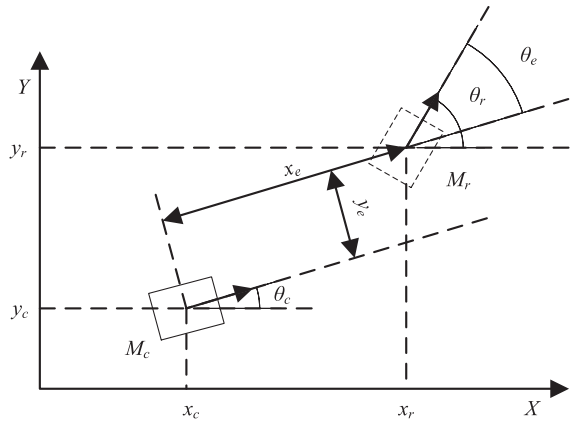

Fig. 4. The trajectory tracking error.

$$\dot{\mathbf{p}}_\mathbf{e} = \begin{pmatrix} \dot{x}_e \\ \dot{y}_e \\ \dot{\theta}_e \end{pmatrix} = \begin{pmatrix} y_e\omega_c - v_c + v_r\cos\theta_e \\ -x_e\omega_c + v_r\sin\theta_e \\ \omega_r - \omega_c \end{pmatrix} \tag{34}$$

where x_e, y_e and θ_e are the errors in the vehicle coordinates, v_c and ω_c are the current actual speed and yaw rate of the host vehicle, and v_r and ω_r are the corresponding reference speed and yaw rate from the reference trajectory.

The purpose of the trajectory-tracking controller is to calculate the control input to make the errors $\mathbf{p_e} = (x_e, y_e, \theta_e)^T$ as small as possible, subject to $\lim_{t\to\infty}\|(x_e, y_e, \theta_e)^T\| = 0$.

On the basis of the Backstepping method, we design our sliding surface using a Lyapunov function. The switching function is

$$\mathbf{s} = \begin{pmatrix} s_1 \\ s_2 \end{pmatrix} = \begin{pmatrix} x_e \\ \theta_e + \arctan(v_r y_e) \end{pmatrix} \tag{35}$$

With the constant reaching law shown in (36) and its variation in continuous form given in (37), we find the control law shown in (39) that makes the tracking error approach zero.

$$\dot{\mathbf{s}} = -\mathbf{k}\ \mathrm{sgn}\ \mathbf{s} \tag{36}$$

$$\dot{s}_i = -k_i\frac{s_i}{|s_i| + \delta_i}, \quad i = 1, 2 \tag{37}$$

$$\dot{\mathbf{s}} = \begin{pmatrix} \dot{s}_1 \\ \dot{s}_2 \end{pmatrix} = \begin{pmatrix} -k_1\frac{s_1}{|s_1|+\delta_1} \\ -k_2\frac{s_2}{|s_2|+\delta_2} \end{pmatrix} = \begin{pmatrix} \dot{x}_e \\ \dot{\theta}_e + \frac{\partial\alpha}{\partial v_r}\dot{v}_r + \frac{\partial\alpha}{\partial y_e}\dot{y}_e \end{pmatrix} = \begin{pmatrix} y_e\omega_c - v_c + v_r\cos\theta_e \\ \omega_r - \omega_c + \frac{\partial\alpha}{\partial v_r}\dot{v}_r + \frac{\partial\alpha}{\partial y_e}(-x_e\omega_c + v_r\sin\theta_e) \end{pmatrix} \tag{38}$$

$$\boldsymbol{q} = \begin{pmatrix} v_c \\ \omega_c \end{pmatrix} = \begin{pmatrix} y_e + v_r\cos\theta_e + k_1\frac{s_1}{|s_1|+\delta_1} \\ \frac{\omega_r + \frac{\partial\alpha}{\partial v_r}\dot{v}_r + \frac{\partial\alpha}{\partial y_e}(v_r\sin\theta_e) + k_2\frac{s_2}{|s_2|+\delta_2}}{1+\frac{\partial\alpha}{\partial y_e}x_e} \end{pmatrix} \tag{39}$$

where $\frac{\partial\alpha}{\partial v_r} = \frac{y_e}{1+(v_r y_e)^2}$ and $\frac{\partial\alpha}{\partial y_e} = \frac{v_r}{1+(v_r y_e)^2}$.

The control law is then converted into an input to the actuators. The desired speed and yaw rate are realized by controlling the torque and the steering wheel, respectively.

$$T = r\left(fmg + \frac{1}{2}C_D A\rho v^2 + m\frac{dv}{dt}\right) \tag{40}$$

$$\delta_{sw} = i_w\delta = i_w\frac{1 + \frac{m}{L^2}\left(\frac{a}{C_r} - \frac{b}{C_f}\right)v^2}{v/L}\omega \tag{41}$$

where r is the dynamic radius of the wheel. f is the friction coefficient. m is the mass of the vehicle. g is the gravitational constant. C_D is the aerodynamic drag factor. A is the frontal area of the vehicle. ρ is the density of air. v is the vehicle speed. δ_{sw} is the steering wheel angle. i_w is the angle transmission rate of the steering system. δ is the steering angle of the front wheels. L is the distance between the front and rear axles. a is the distance between the center of gravity and the front axle. b is the distance between the center of gravity and the rear axle. C_f and C_r are the cornering stiffness of the front and rear wheels, and ω is the yaw rate.

3. Results of simulations and experiments

3.1. Simulations with Simulink and CarSim

To validate the automated lane change maneuver, we employ a simulation platform based on MATLAB/Simulink and CarSim.

The simulation model contains three modules. The trajectory-planning module generates a reference trajectory for an automated lane change that considers safety, comfort and traffic efficiency. The trajectory-tracking module calculates actuator inputs to ensure that the host vehicle travels along the reference trajectory. The CarSim vehicle model can simulate the dynamic characteristics of the vehicle well.

The experimental vehicle is a typical B-class hatchback and its main parameters are listed in Table 1.

In the simulation, we investigate the lane change scenarios shown in Table 2 on a highway with the following assumptions:

(1) only lane change behavior involving the adjacent lanes is considered;
(2) the average speed in the left lane is greater than that in the right lane with 20 km/h;
(3) all vehicles except the host vehicle travel with the average speeds of their lanes.

The key part of the proposed dynamic automated lane change maneuver is the trajectory planning. When we find the optimal lane change time and distance, the lane change reference trajectory can be calculated through (13)–(15). Therefore, a dynamic maneuver can also be used in a normal lane change task, with no threat of collision. The difference between the trajectory planning method proposed here and that of (Papadimitriou and Tomizuka, 2003) is how the lane change time and distance are obtained. Because of this difference, the dynamic automated lane change maneuver can handle the potential collision occurring during the lane change process while the other maneuvers cannot.

The parameters of the planned trajectories for the above eight scenarios are shown in Table 3. The results show that the accelerations, jerks and yaw rates are cooperatively optimized and they are all kept as small as possible to maintain a comfortable lane change.

To simplify the problem enough to illustrate the effectiveness of the dynamic automated lane change maneuver, we assume that an emergency occurs when a potential collision results from too little distance between the host vehicle and another vehicle. To avoid this potential collision, the system calculates another reference trajectory. In the case where no feasible reference trajectory can be found to avoid the potential collision, we plan a reference trajectory that guides the host vehicle back to its original lane with the same trajectory planning method. Therefore, in this section, we will describe some typical lane change scenarios to show how effectively the proposed maneuver deals with emergencies occurring during the lane change process.

(1) An automated lane change on a straight road at high speed from a slower lane to a faster lane

In this scenario, we suppose that the host vehicle travels on a straight road at a speed of 100 km/h and changes from the slower right lane to the faster left lane. After 1.5 s of the lane change, the host vehicle perceives that the distance (13 m) between itself and the following vehicle in the destination lane (F_d) is too short (less than the desired 16.91 m according to the formula (4)) and there is a collision threat. Therefore, we recalculate the reference trajectory from that moment to avoid the potential collision.

A comparison of the dynamic and normal lane change maneuvers is shown in Fig. 5. Here, the normal lane change maneuver is the automated lane change maneuver that is generated at the start of the lane change and its collision avoidance is only based on the situation at the beginning. The normal maneuver cannot update itself after the lane change is initiated. The dynamic maneuver is the automated lane change maneuver that is proposed in this paper. Based on the V2V communication, the dynamic maneuver updates itself to avoid the potential collision during the whole lane change process.

The performance parameters during the dynamic automated lane change maneuver are shown in Table 4. These parameters show that the dynamic maneuver guarantees a safe and comfortable lane change.

Where $a_{x,max}$ is the maximum longitudinal acceleration, $a_{y,max}$ is the maximum lateral acceleration, θ_{max} is the maximum yaw angle, and ω_{max} is the maximum yaw rate.

(2) An automated lane change on a straight road at high speed from a faster lane to a slower lane

In this scenario, we suppose that the host vehicle travels on a straight road at a speed of 100 km/h and changes from the faster left lane to the slower right lane. As similar with the previous situation, there is a potential collision with leading vehicle in the destination lane (L_d) 1.5 s after the normal maneuver starts because of insufficient space between L_d and the host vehicle.

A comparison of lane changes using the two maneuvers is shown in Fig. 6.

Table 1
Main parameters of the experimental vehicle.

Parameter	Unit	Value
Vehicle mass	kg	1271
Distance between CG and front axle	m	1.04
Distance between CG and rear axle	m	1.56
Axle track	m	1.56
Dynamic tire radius	m	0.397
Front cornering stiffness, C_f	N/rad	69679
Rear cornering stiffness, C_r	N/rad	38980

Table 2
Typical lane change scenarios.

Curvature (1/m)	Speed (km/h)	Lane change direction (km/h)	No.
0 (Straight road)	100 (high speed)	(a) from slower lane (100) to faster lane (120)	(1)
		(b) from faster lane (100) to slower lane (80)	(2)
	60 (low speed)	(a) from slower lane (60) to faster lane (80)	(3)
		(b) from faster lane (60) to slower lane (40)	(4)
1/500 (Curved road)	100 (high speed)	(a) from slower lane (100) to faster lane (120)	(5)
		(b) from faster lane (100) to slower lane (80)	(6)
	60 (low speed)	(a) from slower lane (60) to faster lane (80)	(7)
		(b) from faster lane (60) to slower lane (40)	(8)

Table 3
Trajectory parameters for typical lane change scenarios.

No.	$\lvert a_{x,max}\rvert$ (m/s^2)	$\lvert a_{y,max}\rvert$ (m/s^2)	$\lvert j_{x,max}\rvert$ (m/s^3)	$\lvert j_{y,max}\rvert$ (m/s^3)	θ_{max} (deg)	$\lvert \omega_{max}\rvert$ (deg/s)
(1)	1.63	0.53	1.80	0.85	2.15	1.07
(2)	1.46	0.58	1.40	0.99	2.58	1.38
(3)	1.31	0.52	1.00	0.84	3.28	1.68
(4)	1.63	0.58	1.80	0.99	5.19	2.88
(5)	1.16	2.09	2.12	0.85	22.06	4.26
(6)	1.71	1.54	1.59	0.98	17.66	4.00
(7)	1.18	1.16	1.22	0.84	14.29	3.65
(8)	1.59	0.78	1.82	0.99	9.29	4.16

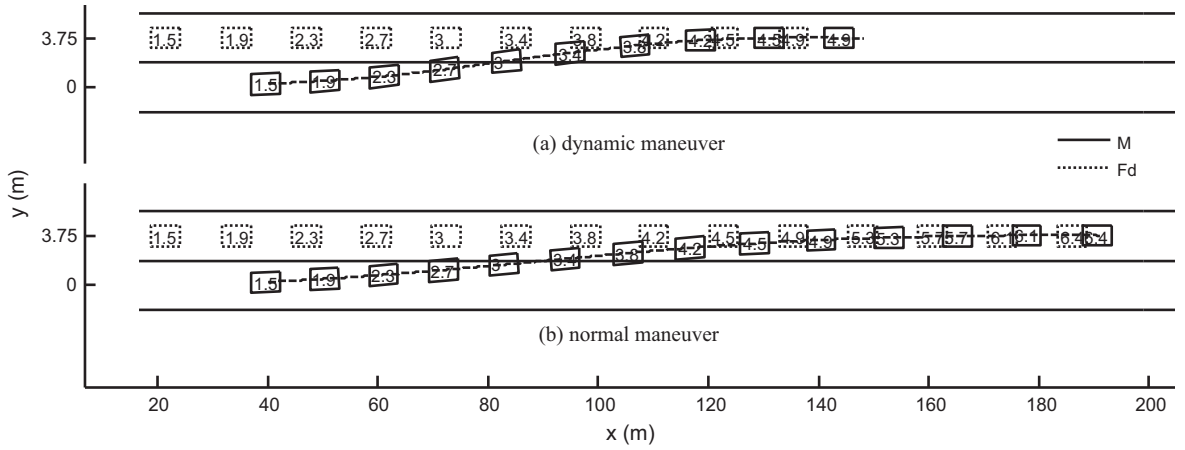

Fig. 5. A comparison of two lane-change processes (high speed, F_d).

Table 4
Performance parameters (high speed, F_d).

$\lvert a_{x,max}\rvert$ (m/s^2)	$\lvert a_{y,max}\rvert$ (m/s^2)	θ_{max} (deg)	$\lvert \omega_{max}\rvert$ (deg/s)
3.48	1.81	3.33	3.43

The performance parameters during the dynamic automated lane change maneuver are shown in Table 5. These parameters show that the dynamic maneuver guarantees a safe and comfortable lane change.

(3) An automated lane change on a straight road at low speed from a slower lane to a faster lane

In this scenario, we suppose that the host vehicle travels on a straight road at a speed of 60 km/h and changes from the slower right lane to the faster left lane. As similar with the first scenario, there is a potential collision with the following vehicle in the destination lane (F_d) 1.5 s after the normal maneuver starts because of insufficient space between F_d and host vehicle.

A comparison of the lane change processes using the two maneuvers is shown in Fig. 7.

The performance parameters during the dynamic automated lane change maneuver are shown in Table 6. These parameters show that the dynamic maneuver guarantees a safe and comfortable lane change.

(4) An automated lane change on a curved road at high speed from a faster lane to a slower lane

In this scenario, we suppose that the host vehicle travels on a curved road at a speed of 100 km/h and changes from the faster left lane to the slower right lane. As in a previous situation, there is a potential collision with the leading vehicle in the destination lane (L_d) 1.5 s after the normal maneuver starts because of insufficient space between L_d and the host vehicle.

A comparison of the lane change processes using the two maneuvers is shown in Fig. 8.

The performance parameters during the dynamic automated lane change maneuver are shown in Table 7. These parameters show that the dynamic maneuver guarantees a safe and comfortable lane change.

(5) An automated lane change on a straight road at high speed from a slower lane to a faster lane

In this scenario, we suppose that the host vehicle travels on a straight road at a speed of 100 km/h and changes from the slower right lane to the faster left lane. 1.5 s after starting the normal lane maneuver, there is insufficient space between the following vehicle in the destination lane (F_d) and the host vehicle to obtain a feasible reference trajectory and to continue the lane change even when a new reference trajectory is calculated. Therefore, a reference trajectory guiding the host vehicle back to its original lane is calculated.

A comparison of the two maneuvers is shown in Fig. 9.

The performance parameters during the dynamic automated lane change maneuver are shown in Table 8. These parameters show that the dynamic maneuver guarantees a safe and comfortable lane change.

From the simulation results for these five typical scenarios, we can say that the dynamic automated lane change maneuver effectively deals with emergencies in different situations, no matter what the shape of the road, the travelling speed and the lane change direction are.

3.2. A hardware-in-loop experiment with a driving simulator

In addition to the simulations performed using Simulink and CarSim, we set up the hardware-in-loop (HIL) experimental platform based on the driving simulator to further validate our automated lane change maneuver. The driving simulator is based on real vehicle and it can simulate the driver's view and driver's perception. The HIL experimental platform is a close-loop system of driver–vehicle–road. It can simulate the dynamic response of the real vehicle. The experimental configuration is shown in Fig. 10. The driving simulator consists of a vehicle-motion simulation system, a visual environment simulation system, an acoustic environment simulation system, a driving simulation system, a vehicle-dynamics simulation model, a

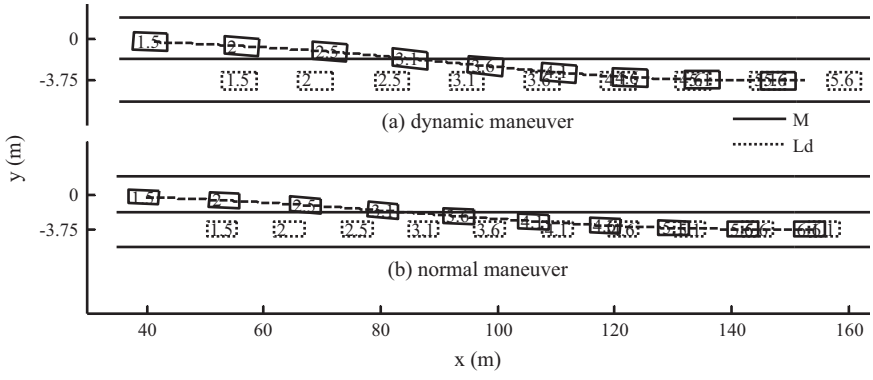

Fig. 6. A comparison of two lane-change processes (high speed, L_d).

Table 5
Performance parameters (high speed, L_d).

$\|a_{x,max}\|$ (m/s^2)	$\|a_{y,max}\|$ (m/s^2)	θ_{max} (deg)	$\|\omega_{max}\|$ (deg/s)
3.53	0.81	3.35	2.80

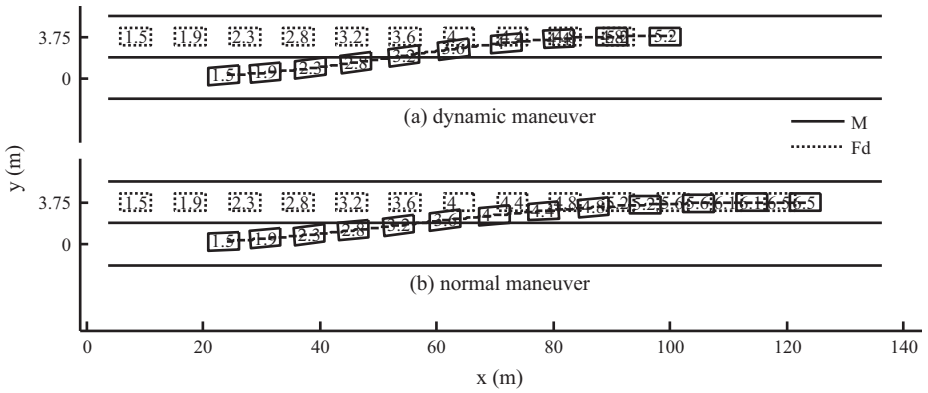

Fig. 7. A comparison of two lane-change processes (low speed, F_d).

Table 6
Performance parameters (low speed, F_d).

$\|a_{x,max}\|$ (m/s^2)	$\|a_{y,max}\|$ (m/s^2)	θ_{max} (deg)	$\|\omega_{max}\|$ (deg/s)
4.97	0.57	3.33	1.93

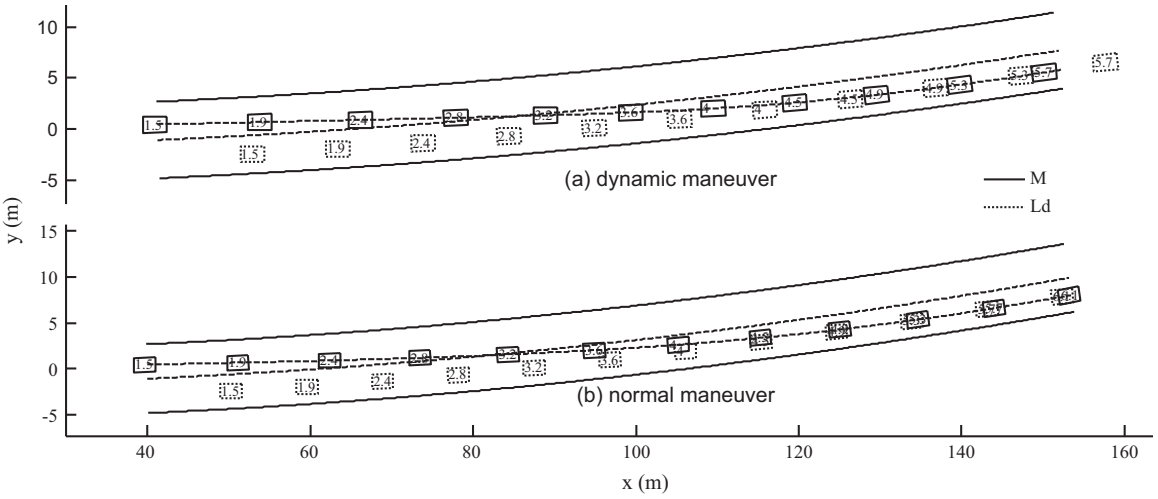

Fig. 8. A comparison of two lane-change processes (high speed, L_d, curved road).

Table 7
Performance parameters (high speed, L_d, curved road).

$\|a_{x,max}\|$ (m/s^2)	$\|a_{y,max}\|$ (m/s^2)	θ_{max} (deg)	$\|\omega_{max}\|$ (deg/s)
3.52	1.11	8.93	2.87

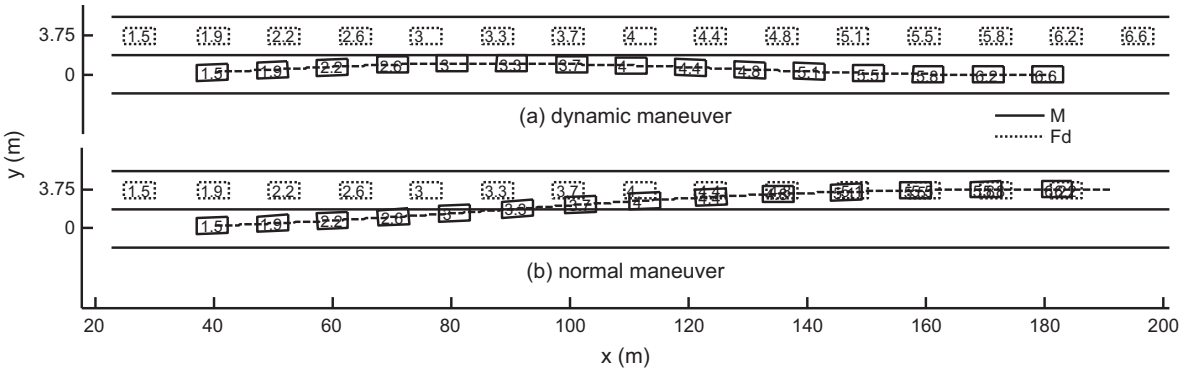

Fig. 9. A comparison of two lane-change processes (high speed, F_d, back to original lane).

Table 8
Performance parameters (high speed, F_d, back to original lane).

$\|a_{x,max}\|$ (m/s^2)	$\|a_{y,max}\|$ (m/s^2)	θ_{max} (deg)	$\|\omega_{max}\|$ (deg/s)
3.48	0.93	1.55	1.98

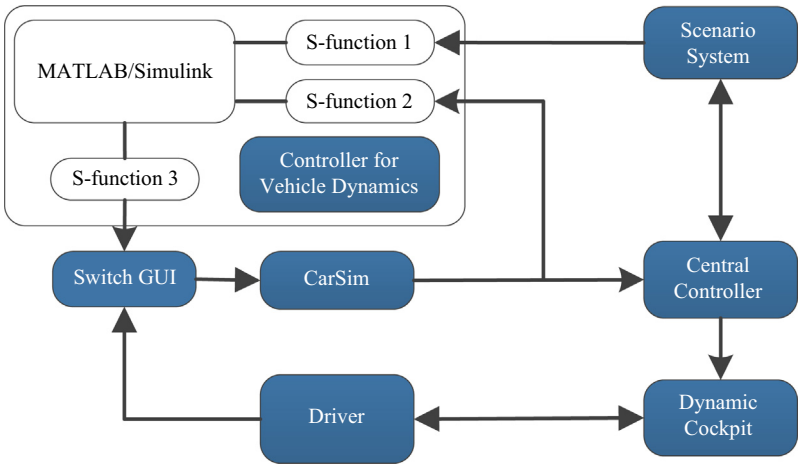

(a) A diagram of the platform

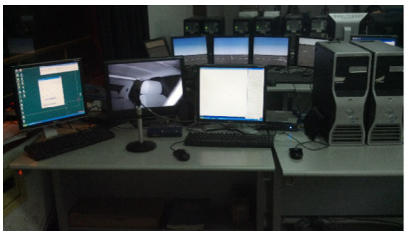

(b) The central controller

(c) The dynamic cockpit

Fig. 10. The HIL experimental platform.

central control platform and so on. The HIL experimental platform can be controlled through Simulink and it can simulate the motion of a vehicle with six degrees of freedom.

The main experimental results for the four straight-road scenarios described above are shown in Table 9. These parameters show that the acceleration, jerk, sideslip angle, yaw angle and yaw rate are limited to a suitable range and a comfortable lane change is guaranteed. The results of the HIL experiment differ slightly from those of the simulation, which means the fluctuation is larger.

Table 9
The critical parameters for the typical lane change scenarios.

No.	$\lvert a_{x,max}\rvert$ (m/s^2)	$\lvert a_{y,max}\rvert$ (m/s^2)	$\lvert\beta_{max}\rvert$ (deg)	θ_{max} (deg)	$\lvert\omega_{max}\rvert$ (deg/s)
(1)	1.73	0.54	0.34	2.20	1.97
(2)	3.08	0.62	0.35	2.61	2.06
(3)	1.39	0.63	0.42	3.26	1.39
(4)	3.55	1.53	2.44	5.11	3.86

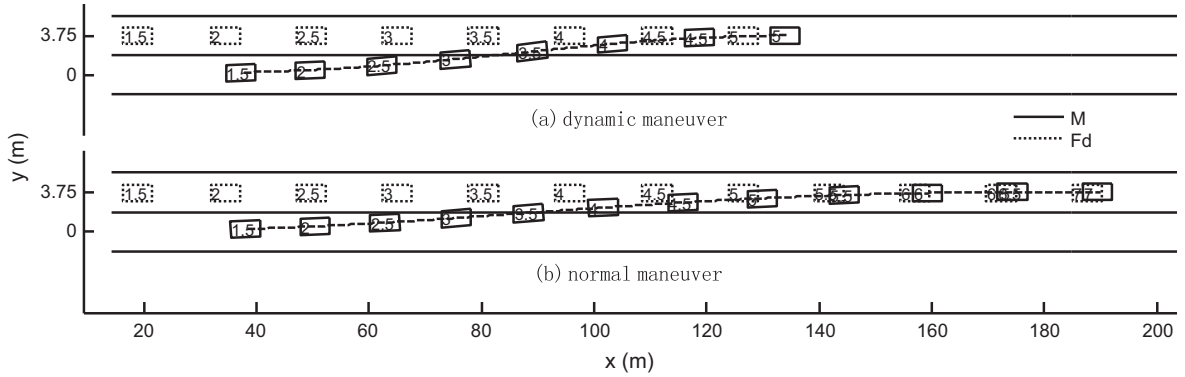

Fig. 11. A comparison of two lane-change processes for the HIL experiment (high speed, F_d).

Table 10
Performance parameters for the HIL experiment (high speed, F_d).

$\lvert a_{x,max}\rvert$ (m/s^2)	$\lvert a_{y,max}\rvert$ (m/s^2)	θ_{max} (deg)	$\lvert\omega_{max}\rvert$ (deg/s)
2.59	1.48	3.16	2.94

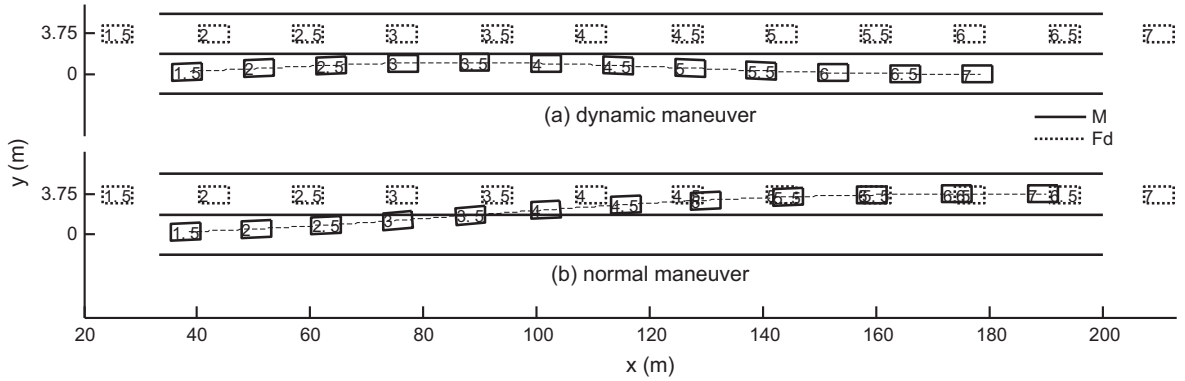

Fig. 12. A comparison of two lane-change processes in the HIL experiment (high speed, F_d, back to original lane).

As we can see from the simulation results, the proposed dynamic automated lane change maneuver has the same effect under different scenarios. The experimental results here do show the same. Therefore, in this section, we display only two of the above scenarios to illustrate the feasibility of the dynamic automated lane change maneuver in the HIL experiment to avoid redundancy.

Fig. 11 shows the result of the HIL experiment when the host vehicle travels at a speed of 100 km/h and changes from the slower right lane to the faster left lane. During the lane change, the distance between the host vehicle and F_d is insufficient because there is a vehicle cutting in behind the host vehicle in the destination lane 1.5 s after the lane change has begun; therefore, the reference trajectory is updated according to the dynamic automated lane change maneuver. We find the same result in the HIL experiment and in the simulation.

The performance parameters during the dynamic automated lane change maneuver are shown in Table 10. These parameters show that the dynamic maneuver guarantees a safe and comfortable lane change.

Table 11
Performance parameters for the HIL experiment (high speed, F_d, back to original lane).

$\lvert a_{x,max}\rvert$ (m/s^2)	$\lvert a_{y,max}\rvert$ (m/s^2)	θ_{max} (deg)	$\lvert \omega_{max}\rvert$ (deg/s)
0.55	0.83	1.47	1.79

Fig. 12 shows the result of the HIL experiment in which the host vehicle travels at a speed of 100 km/h and changes from the slower right lane to the faster left lane. During the lane change, the distance between the host vehicle and F_d is so small that there is no feasible reference trajectory in which to continue the lane change. Therefore, the host vehicle is guided back to its original lane. We find the same result in the HIL experiment and in the simulation.

The performance parameters during the dynamic automated lane change maneuver are shown in Table 11. These parameters show that the dynamic maneuver guarantees a safe and comfortable lane change.

4. Conclusions

In this paper, we have conducted research into automated lane change maneuver to overcome the existing shortcomings in this area. Earlier studies have resolved the problem of changing lanes without other vehicles nearby and with potential collisions that can be detected initially, but have seldom considered potential collisions that appear during the lane change. We have proposed a dynamic automated lane change maneuver based on vehicle-to-vehicle communication and designed its key technologies.

The proposed dynamic automated lane change maneuver allows the host vehicle to avoid potential collisions resulting from variations in the states of other vehicles during the lane change. Therefore, the maneuver allows the host vehicle to avoid many types of potential collisions by adjusting the reference trajectory to maintain sufficient distance between the host vehicle and other vehicles.

The idea of converting trajectory planning into a constrained optimization problem to plan various reference trajectories efficiently is validated. With a cost function that includes constraints of the comfort and the traffic efficiency and safety, the results of the constrained optimization problem satisfy the multi-objective demands on the reference trajectory.

The proposed trajectory planning method can calculate a reference trajectory either when the other vehicles' states are constant or when they vary compared to the beginning of the lane change during the lane change process. It can update the lane change trajectory or plan a new trajectory back to the original lane. The proposed method is an all-purpose trajectory planning method that can be applied to various automated lane change scenarios.

Until now, we have proposed a complete automated lane change maneuver. In the future, we would like to optimize the maneuver to improve the passenger comfort on curved road by considering the yaw rate. As the quality of the V2V communication is so important for the practical performance of the proposed automated lane change maneuver, that we will also conduct research on the performance of V2V communication. To strengthen the robustness of our maneuver, the uncertainties are also our next focus. Finally, we would like to establish an experimental platform based on real vehicles to conduct field tests.

Acknowledgments

This research was funded by the National Key Fundamental Research Program of China (2011CB711204) and was supported by the Collaborative Innovation Center for Electric Vehicles in Beijing.

References

Adell, E., Varhelyi, A., Dalla Fontana, M., 2011. The effects of a driver assistance system for safe speed and safe distance – a real-life field study. Transport. Res. Part C: Emerg. Technol. 19 (1), 145–155.
Ammoun, S., Nashashibi, F., 2010. Design and efficiency measurement of cooperative driver assistance system based on wireless communication devices. Transport. Res. Part C: Emerg. Technol. 18 (3), 408–428.
Ammoun, S., Nashashibi, F., Laurgeau, C., 2007. An analysis of the lane changing manoeuvre on roads: the contribution of inter-vehicle cooperation via communication. In: Intelligent Vehicles Symposium, Istanbul, 13–15 June 2007, pp. 1095–1100.
Carbaugh, J., Godbole, D.N., Sengupta, R., 1998. Safety and capacity analysis of automated and manual highway systems. Transport. Res. Part C: Emerg. Technol. 6 (1–2), 69–99.
Chee, W., Tomizuka, M., 1994a. Vehicle Lane Change Maneuver in Automated Highway Systems. California Partners for Advanced Transit and Highways (PATH). California Partners for Advanced Transportation Technology, UC Berkeley.
Chee, W., Tomizuka, M., 1994b. Lane change maneuver of automobiles for the intelligent vehicle and highway system (IVHS). Am. Control Conf. 3, 3586–3587.
Chee, W., Tomizuka, M., Patwardhan, S., Zhang, W.-B., 1995. Lane change maneuvers for automated highway systems: control, estimation algorithms and preliminary experimental study. In: Proceedings of the 1995 ASME International Mechanical Engineering Congress and Exposition, pp. 79–84.
Chee, W., Tomizuka, M., Patwardhan, S., Zhang, W.-B., 1995. Experimental study of lane change maneuver for AHS applications. In: Proceedings of the 1995 American Control Conference. Part 1 (of 6), pp. 139–143.
Fraedrich, E., Lenz, B., 2014. Automated driving – individual and societal aspects. Transport. Res. Rec.: J. Transport. Res. Board 2416, 64–72.
Gallagher, B., Akatsuka, H., Suzuki, H., 2006. Wireless communications for vehicle safety: radio link performance and wireless connectivity methods. IEEE Veh. Technol. Mag. 1 (4), 4–24.

Girault, A., 2004. A hybrid controller for autonomous vehicles driving on automated highways. Transport. Res. Part C: Emerg. Technol. 12 (6), 421–452.
Greg, L., 2014. Caltrans Interests in Connected/Automated Vehicles. <http://www.westernite.org/Sections/sbr/presentations/RSBITE-January2014.pdf> (access: 10, January 2015).
Guan, W., He, J., Bai, L., Tang, Z., 2011. Adaptive Congestion Control of DSRC Vehicle Networks for Collaborative Road Safety Applications. Local Computer Networks (LCN), Bonn, 4–7 October 2011, pp. 913–917.
Hatipoglu, C., Ozguner, U., Unyelioglu, K.A., 1995. On optimal design of a lane change controller. In: Proceedings of the Intelligent Vehicles' 95 Symposium, pp. 436–441.
Hatipoglu, C., Ozguner, U., Unyelioglu, K.A., 1997. Advanced automatic lateral control schemes for vehicles on highways. In: Proceedings of the 13th World Congress-International Federation of Automatic Control, pp. 477–482.
Hidas, P., 2002. Modelling lane changing and merging in microscopic traffic simulation. Transport. Res. Part C: Emerg. Technol. 10 (5–6), 351–371.
Hu, J., Kong, L., Shu, W., Wu, M., 2012. Scheduling of connected autonomous vehicles on highway lanes. In: Global Communications Conference, Anaheim, CA, 3–7 December 2012, pp. 5556–5561.
Hult, R., Tabar, R.S., 2013. Path Planning for Highly Automated Vehicles. Master Thesis, Chalmers University of Technology.
Jula, H., Kosmatopoulos, E.B., Ioannou, P.A., 2000. Collision avoidance analysis for lane changing and merging. IEEE Trans. Veh. Technol. 49 (6), 2295–2308.
Kato, S., Tsugawa, S., Tokuda, K., Matsui, T., Fujii, H., 2002. Vehicle control algorithms for cooperative driving with automated vehicles and intervehicle communications. IEEE Trans. Intell. Transport. Syst. 3 (3), 155–161.
Liu, T., Wang, Y., Wenjuan, E., Tian, D., Yu, G., Wang, J., 2012. Vehicle collision warning system and algorithm at intersection under internet-connected vehicles environment. In: Proceedings of 12th COTA International Conference of Transportation Professionals: Multimodal Transportation Systems – Convenient, Safe, Cost-Effective, Efficient, pp. 1177–1185.
Misener, J.A., 2008. Wireless-enabled Safety Services in California: VII California, Intersection Safety and Other Emerging Innovations. SAE Technical Paper.
Nelson, W., 1989. Continuous-curvature paths for autonomous vehicles. In: Proceedings of 1989 IEEE International Conference on Robotics and Automation, vol. 3, pp. 1260–1264.
Papadimitriou, I., Tomizuka, M., 2003. Fast lane changing computations using polynomials. In: Proceedings of the 2003 American Control Conference, vol. 1, pp. 48–53.
Sledge Jr., N.H., Marshek, K.M., 1997. Comparison of Ideal Vehicle Lane-change Trajectories. SAE Technical Paper.
Tian, D., Leung, V.C.M., 2011. Analysis of broadcasting delays in vehicular ad hoc networks. Wireless Commun. Mobile Comput. 11 (11), 1433–1445.
Tian, D., Luo, H., Zhou, J., Wang, Y., Yu, G., Xia, H., 2013. A self-adaptive V2V communication system with DSRC. In: 2013 IEEE International Conference on Green Computing and Communications and IEEE Internet of Things and IEEE Cyber, Physical and Social Computing, Beijing, China, 20–23 August 2013, pp. 1528–1532.
Tian, D., Zhou, J., Wang, Y., Xia, H., Yi, Z., Liu, H., 2014. Optimal epidemic broadcasting for vehicular ad hoc networks. Int. J. Commun. Syst. 27 (9), 1220–1242.
Tideman, M., Van Der Voort, M.C., Van Arem, B., 2010. A new scenario based approach for designing driver support systems applied to the design of a lane change support system. Transport. Res. Part C: Emerg. Technol. 18 (2), 247–258.
Wan, L., Raksincharoensak, P., Maeda, K., Nagai, M., Kimpara, H., Nakahira, Y., Iwamoto, M., Rowson, S., Duma, S., Avery, P.A., 2011. Lane change behavior modeling for autonomous vehicles based on surroundings recognition. Int. J. Autom. Eng. 2 (2), 7–12.
Wang, Y., Wenjuan, E., Tang, W., Tian, D., Lu, G., Yu, G., 2013. Automated on-ramp merging control algorithm based on internet-connected vehicles. IET Intell. Transport Syst. 7 (4), 371–379.
Wang, M., Hoogendoorn, S.P., Daamen, W., van Arem, B., Happee, R., 2015. Game theoretic approach for predictive lane-changing and car-following control. Transport. Res. Part C: Emerg. Technol. 58 (Part A), 73–92.
Williams, T., Alves, P., Lachapelle, G., Basnayake, C., 2012. Evaluation of GPS-based methods of relative positioning for automotive safety applications. Transport. Res. Part C: Emerg. Technol. 23, 98–108.
Zheng, Z., 2014. Recent developments and research needs in modeling lane changing. Transport. Res. Part B: Methodol. 60, 16–32.